

RESEARCH ARTICLE

# Differential Gene Expression Patterns in Chicken Cardiomyocytes during Hydrogen Peroxide-Induced Apoptosis

Chunyun Wan<sup>1,2</sup>, Jinmei Xiang<sup>1,3</sup>, Youwen Li<sup>1</sup>, Dingzong Guo<sup>1\*</sup>

**1** College of Veterinary Medicine, Huazhong Agricultural University, Wuhan, Hubei, People's Republic of China, **2** College of Animal Science, Yangtze University, Jingzhou, Hubei, People's Republic of China, **3** Hubei Vocational College Of Bio-Technology, Wuhan, Hubei, People's Republic of China

✉ These authors contributed equally to this work.

\* [hlgdz@163.com](mailto:hlgdz@163.com)



## Abstract

Hydrogen peroxide (H<sub>2</sub>O<sub>2</sub>) is both an exogenous and endogenous cytotoxic agent that can reliably induce apoptosis in numerous cell types for studies on apoptosis signaling pathways. However, little is known of these apoptotic processes in myocardial cells of chicken, a species prone to progressive heart failure. Sequencing of mRNA transcripts (RNA-Seq) allows for the identification of differentially expressed genes under various physiological and pathological conditions to elucidate the molecular pathways involved, including cellular responses to exogenous and endogenous toxins. We used RNA-seq to examine genes differentially expressed during H<sub>2</sub>O<sub>2</sub>-induced apoptosis in primary cultures of embryonic chicken cardiomyocytes. Following control or H<sub>2</sub>O<sub>2</sub> treatment, RNA was extracted and sequencing performed to identify novel transcripts up- or downregulated in the H<sub>2</sub>O<sub>2</sub> treatment group and construct protein–protein interaction networks. Of the 19,268 known and 2,160 novel transcripts identified in both control and H<sub>2</sub>O<sub>2</sub> treatment groups, 4,650 showed significant differential expression. Among them, 55.63% were upregulated and 44.37% downregulated. Initiation of apoptosis by H<sub>2</sub>O<sub>2</sub> was associated with upregulation of *caspase-8*, *caspase-9*, and *caspase-3*, and downregulation of anti-apoptotic genes *API5* and *TRIA1*. Many other differentially expressed genes were associated with metabolic pathways (including ‘Fatty acid metabolism’, ‘Alanine, aspartate, and glutamate metabolism’, and ‘Biosynthesis of unsaturated fatty acids’) and cell signaling pathways (including ‘PPAR signaling pathway’, ‘Adipocytokine signaling pathway’, ‘TGF-β signaling pathway’, ‘MAPK signaling pathway’, and ‘p53 signaling pathway’). In chicken cardiomyocytes, H<sub>2</sub>O<sub>2</sub> alters the expression of numerous genes linked to cell signaling and metabolism as well as genes directly associated with apoptosis. In particular, H<sub>2</sub>O<sub>2</sub> also affects the biosynthesis and processing of proteins and unsaturated fatty acids. These results highlight the value of RNA-seq for revealing unexpected molecular contributors to oxidative stress responses, thereby identifying novel potential therapeutic targets.

## OPEN ACCESS

**Citation:** Wan C, Xiang J, Li Y, Guo D (2016) Differential Gene Expression Patterns in Chicken Cardiomyocytes during Hydrogen Peroxide-Induced Apoptosis. PLoS ONE 11(1): e0147950. doi:10.1371/journal.pone.0147950

**Editor:** Rodrigo Franco, University of Nebraska-Lincoln, UNITED STATES

**Received:** August 18, 2015

**Accepted:** January 11, 2016

**Published:** January 25, 2016

**Copyright:** © 2016 Wan et al. This is an open access article distributed under the terms of the [Creative Commons Attribution License](https://creativecommons.org/licenses/by/4.0/), which permits unrestricted use, distribution, and reproduction in any medium, provided the original author and source are credited.

**Data Availability Statement:** All relevant data are within the paper and its Supporting Information files.

**Funding:** This work was supported by preliminary research project of Huazhong agricultural university (52209-814112). The funders had no role in study design, data collection and analysis, decision to publish, or preparation of the manuscript.

**Competing Interests:** The authors have declared that no competing interests exist.

## Introduction

Cell apoptosis was first described in 1972 [1] and soon thereafter implicated in myocardial cell death associated with heart failure [2]. Hydrogen peroxide (H<sub>2</sub>O<sub>2</sub>) has well known cytotoxic effects. It is not only a common exogenous toxin, but is produced endogenously (e.g., by superoxide dismutase), which can lead to cellular apoptosis. Thus, it is widely used to induce apoptosis in toxicology research [3–5]. Myocardial cells are terminally differentiated; if these cells undergo apoptosis, they are not regenerated, leading to a progressive reduction in overall heart function and possible heart failure [2]. Thus, describing the mechanisms of apoptosis in cardiomyocytes is critical for understanding the pathogenesis of heart failure and for developing ameliorative treatments. Cardiomyocyte apoptosis and heart failure are common in chickens. Many strains of rapidly growing chickens are particularly susceptible to cardiomyocyte apoptosis and progressive of rapidly growing chickens are susceptible to heart disease, including heart failures to see if etnclude context-aheart failure as a result of diseases such as broiler pulmonary hypertension syndrome [6].

The sequencing of mRNA transcripts (termed RNA sequencing or RNA-Seq) is a maturing technology now widely used for the identification of differentially expressed genes, both known and without prior annotations [7]. While RNA-seq has been conducted to examine the mechanisms of resistance to *Campylobacter jejuni* colonization in chickens [8], it has not been applied to study apoptotic mechanisms in chicken myocardial cells. We induced apoptosis in chicken myocardial cells using H<sub>2</sub>O<sub>2</sub> [5, 9] and identified differentially expressed genes by 100-bp paired-end reads using the Illumina HiSeq 2000 platform. In the late stage chicken embryo, heart development is nearly complete, and the number of myocardial cells rarely increases. Thus, primary cells isolated at this stage can exhibit the signaling responses of mature cardiomyocytes [10–12].

The aims of this study are threefold: (1) to identify the molecular signaling pathways involved in chicken cardiomyocyte apoptosis and repression of apoptosis, (2) to describe other changes in gene expression associated with the cytotoxicity of hydrogen peroxide, and (3) to evaluate the potential of RNA-seq for aims (1) and (2).

## Materials and Methods

### Ethics statement

This study was approved by the Animal Care and Use Committee of Hubei Province, China. All animal procedures were performed according to the guidelines developed by China's Council on Animal Care.

### Isolation of chicken primary embryonic cardiomyocytes and induction of apoptosis

Monolayer cultures of embryonic chicken cardiomyocytes were prepared by the methods of DeHaan [13] with some modifications. Briefly, White Leghorn eggs were obtained from Beijing Merial Vital Laboratory Animal Technology (Beijing, China). At embryonic day 14 (E14), embryos were removed and decapitated in a Petri dish filled with Medium 199/EBSS (HyClone, Logan, Utah, USA) supplemented with 3% fetal bovine serum (FBS, Gibco, Grand Island, New York, USA). Ventricular tissues were isolated, pooled, and treated with 0.05% trypsin-EDTA to obtain a cell suspension as described [14]. We used the differential attachment technique to obtain high purity cells after 0.5 h of incubation. Cells were incubated in growth medium (Medium 199/EBSS containing 10% FBS) at 37°C under a 5% CO<sub>2</sub> atmosphere. Cultures were washed three times at 8, 24, and 48 h to remove dead and dying cells. The serum concentration

in the medium was then changed from growth (10%) to maintenance (2%) conditions, and incubation was continued for 36 h. The cells were then divided into two groups: a control group and an experimental group treated with 0.2 mM H<sub>2</sub>O<sub>2</sub> for 10 h. The H<sub>2</sub>O<sub>2</sub> dose and exposure time were determined by prior testing and by referencing previous studies [3, 4, 15]. The degree of apoptosis was estimated by DAPI staining. The control group was treated in the same way but with omission of H<sub>2</sub>O<sub>2</sub>. All individual treatments were repeated twice; replicates were named \_1 and \_2, respectively (e.g., H\_1 and H\_2). The RNA sample obtained from each replicate was bi-directionally sequenced, for four sequencing results per sample (named accordingly as H\_1\_1, H\_1\_2, H\_2\_1, and H\_2\_2).

### RNA sample collection and preparation

Total RNA was extracted using standard protocols (TRIzol, Invitrogen, CA, USA) and treated with DNase to remove any potential genomic DNA contamination. The quality of RNA was monitored by electrophoresis on 1% agarose gels. RNA purity and concentration were checked using a NanoPhotometer spectrophotometer (Implen, CA, USA) and Qubit RNA Assay Kit in a Qubit 2.0 Fluorometer (Life Technologies, CA, USA). RNA integrity was assessed using the Bioanalyzer 2100 system (Agilent Technologies, CA, USA).

### Library preparation for transcriptome sequencing

After total RNA extraction, mRNA was purified using poly-T oligo-attached magnetic beads [8]. Briefly, 3 µg of RNA was used as the input for each RNA sample preparation. Sequencing libraries were generated using a NEBNext Ultra RNA Library Prep Kit (Illumina, NEB, USA) following the manufacturer's instructions. Index codes were assigned to attribute the sequences to each sample.

Clustering of the index-coded samples was performed on a cBot Cluster Generation System (Illumina) according to the manufacturer's instructions. After cluster generation, the library preparations were sequenced on an Illumina HiSeq 2000 platform, and 100-bp paired-end reads were generated [16].

### Sequencing quality control and reads mapping to the reference genome

After sequencing, raw data in fastq format were first processed through in-house perl scripts. In this step, clean data were obtained by removing low-quality reads and reads containing the adapter sequence or poly-N. At the same time, Q20, Q30, and the GC content of the clean data were calculated. All subsequent analyses were based on these clean datasets.

Reference genome and gene model annotation files were directly downloaded from the Genome website ([http://www.ncbi.nlm.nih.gov/genome/111?project\\_id=10808](http://www.ncbi.nlm.nih.gov/genome/111?project_id=10808)). An index of the reference genome was built using Bowtie v2.0.6, and paired-end clean reads were aligned to the reference genome using TopHat v2.0.9 [16].

### Quantification of gene expression levels

The reads mapped to each gene were counted by HTSeq v0.5.4p3. The RPKM (reads per kilobase of the exon model per million mapped reads) of each gene was then calculated based on gene length and read counts mapped. This method considers the effects of sequencing depth and gene length for the read counts and is currently the most reliable method for estimating gene expression levels [14].

## Alternative splicing and differential expression analysis

Alternative splicing was determined by Cufflinks 2.1.1 and ASprofile 1.0 software. Differential expression analysis was performed using the DESeq R package (1.10.1). DESeq provides statistical methods for determining differential expression in digital gene expression data using a model based on the negative binomial distribution. The resulting P-values were adjusted using Benjamini and Hochberg's approach for controlling the false discovery rate; that is, genes with an adjusted  $P < 0.05$  by DESeq were classified as differentially expressed. Corrected P values of 0.005 and log<sub>2</sub> (fold change) values of 1 were set as the threshold for significant differential expression.

## GO and KEGG enrichment analysis of differentially expressed genes

After functional annotation, genes were further classified by Gene Ontology (GO) assignments. GO enrichment analysis of differentially expressed genes was performed using the GOrse R package, in which gene length bias was corrected. GO terms with corrected  $P < 0.05$  were considered significantly enriched in differentially expressed genes [17].

The Kyoto Encyclopedia of Genes and Genomes (KEGG) is a database resource for the hierarchical categorization of genes and gene groups identified from genome sequencing and other high-throughput methods (<http://www.genome.jp/kegg/>). We used KOBAS software to test the statistical enrichment of differentially expressed genes in KEGG pathways [18, 19].

## Novel transcript prediction and alternative splicing analysis

The Cufflinks v2.1.1 Reference Annotation Based Transcript (RABT) assembly method was used to construct and identify both known and novel transcripts from the TopHat alignment results. Alternative splicing events were classified into 12 basic types by ASprofile v1.0. The number of AS events was estimated separately in each sample.

## Results

### Induction of apoptosis in chicken primary embryonic cardiomyocytes

We obtained high-purity myocardial cells from chicken embryonic ventricle. Isolated cells beat rhythmically and were immunopositive for  $\alpha$ -actin. Hydrogen peroxide (0.2 mM for 10 h) induced substantial apoptosis as determined by DAPI staining (S1 Fig).

### Sequencing quality control

After RNA sequencing, we assessed the quality of the data. The Q20, Q30, and GC content in the clean data were calculated (Table 1). Alignments between reads and the reference genome are presented in S1 Table. Replicates of each sample were sequenced, and the correlations between replicates are shown in Fig 1.

## Alternative splicing and differential expression analysis

Alternative splicing (AS) analysis was performed using Cufflinks 2.1.1 and ASprofile 1.0. The alternative splicing event statistics are shown in Fig 2. The most common AS types were TSS (alternative 5' first exon) and TTS (alternative 3' last exon). We found some genes with more than five AS types.

To assess global transcriptional changes associated with apoptosis induction, we applied previously described methods [14] to identify differentially expressed genes from the normalized data. The results showed that 4,650 genes were significantly differentially expressed

**Table 1. Major characteristics of RNA-seq in the H<sub>2</sub>O<sub>2</sub> (H) and Control group.**

Sample name	Raw reads	Clean reads	Clean bases	Error rate(%)	Q20(%) <sup>▲</sup>	Q30(%) <sup>▲</sup>	GC content(%) <sup>★</sup>
Control_1_1	61286178	57687170	5.77G	0.03	97.15	91.50	53.26
Control_1_2	61286178	57687170	5.77G	0.04	96.03	89.60	53.32
Control_2_1	57289438	53642113	5.36G	0.04	97.03	91.19	54.04
Control_2_2	57289438	53642113	5.36G	0.04	95.75	88.93	54.09
H_1_1	59514696	56406015	5.64G	0.03	97.35	91.95	52.67
H_1_2	59514696	56406015	5.64G	0.04	96.30	90.12	52.73
H_2_1	62578501	59247377	5.92G	0.03	97.34	92.00	53.19
H_2_2	62578501	59247377	5.92G	0.04	96.39	90.34	53.24

<sup>▲</sup>Q20(%) and Q30(%) are the percentages of reads with Phred quality scores >20 and >30, respectively.

<sup>★</sup> GC content(%) is G+C bases as a percentage of total bassese.

doi:10.1371/journal.pone.0147950.t001

between control and H<sub>2</sub>O<sub>2</sub>-treated cultures. A volcano plot of differential gene expression (Fig 3) shows that 55.63% of all differentially expressed genes were upregulated and 44.37% downregulated.

### Validation of differential gene expression data by qPCR

To validate the differentially expressed genes identified by sequencing, we selected 18 genes for qPCR confirmation, including 8 downregulated genes (*AMPK*, *EGLN1*, *FGF10*, *FOXO3*, *GHOX4.7*, *TGFBR*, *NF-κB*, and *MAPK*) and 10 upregulated genes (*CASP8*, *CASP9*, *CASP3*, *BAK1*, *TNFRSF1A*, *Bcl*, *Bcl2*, *CytC*, *P53*, and *XIAP*). The primers for the qPCR assays are shown in S2 Table. For the selected gene population, there was a strong correlation between RNA-Seq and qPCR results ( $r^2 = 0.9573$ ) (Fig 4), confirming the reliability of differential expression analysis using RNA-Seq.

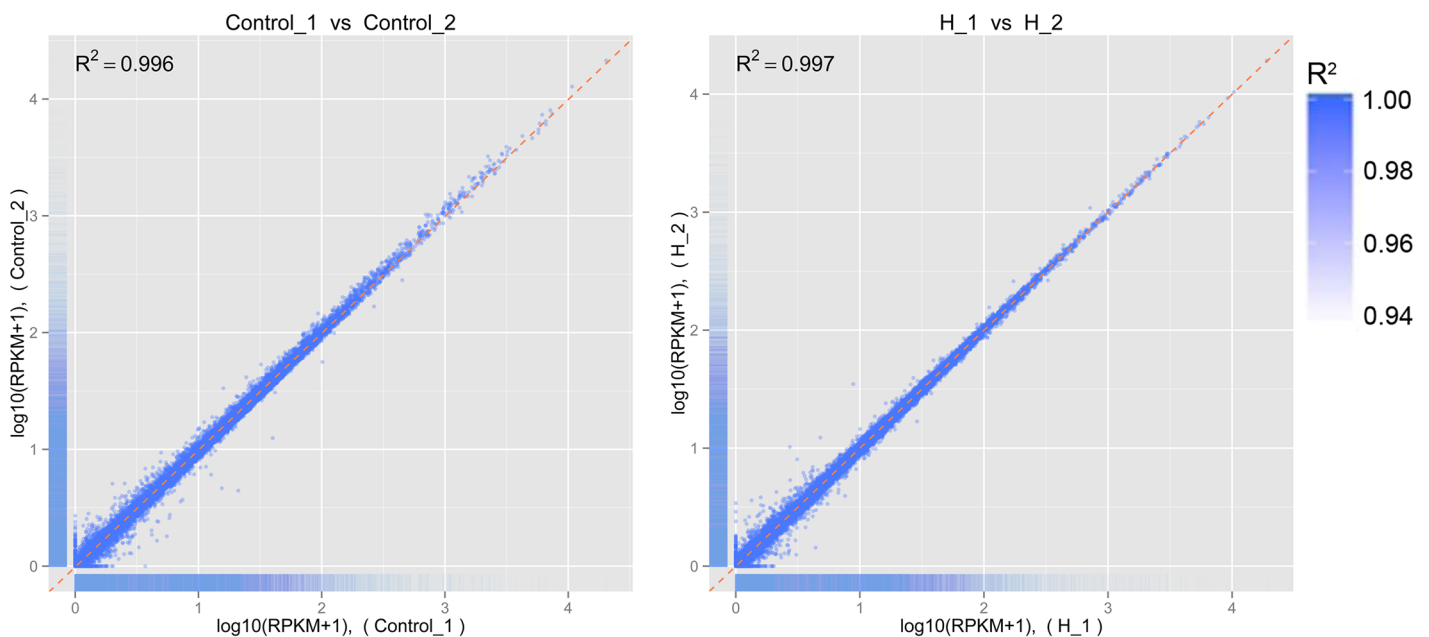


**Fig 1. Correlations among technical replicates in each group.** R<sup>2</sup>: square of the Pearson correlation coefficient.

doi:10.1371/journal.pone.0147950.g001

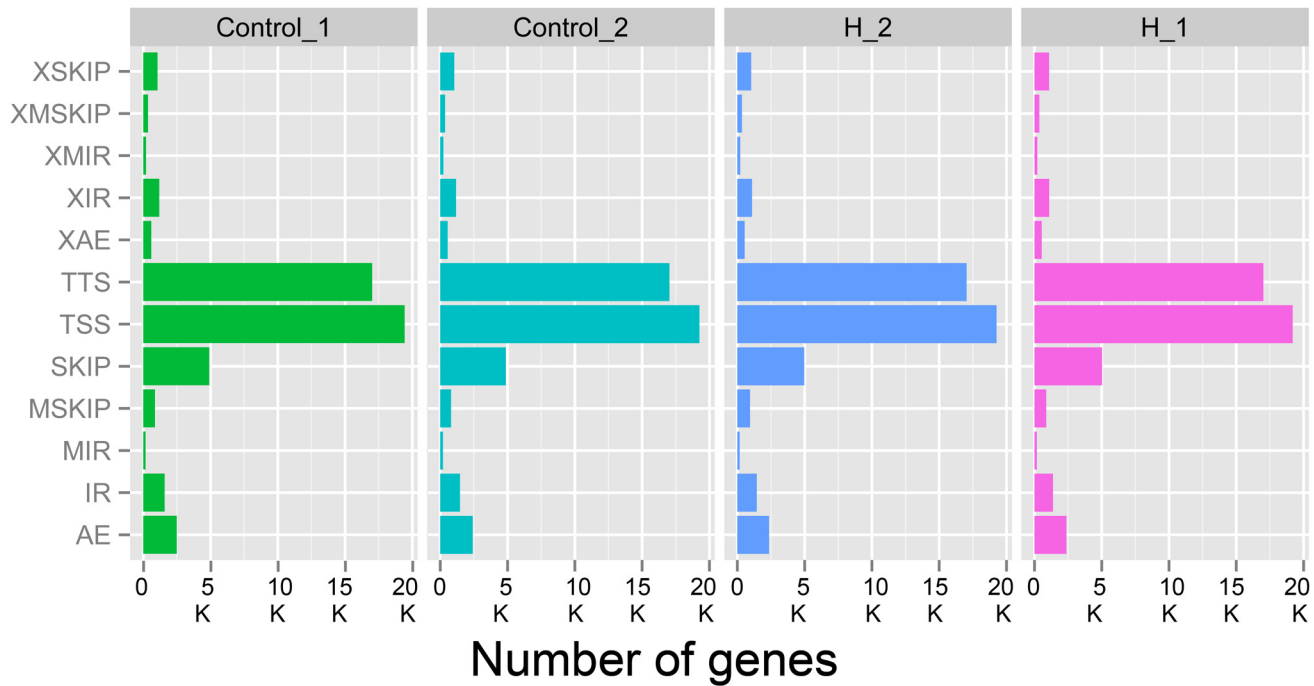


**Fig 2. Statistics of the different alternative splicing events.** The abbreviations indicate the different types of alternative splicing events as follows: SKIP: skipped exon; XSKIP: approximate SKIP; MSKIP: multi-exon SKIP; XMSKIP: approximate MSKIP; IR: intron retention; MIR: multi-IR; XMIR: approximate MIR; XIR: approximate IR; AE: alternative exon ends; XAE: approximate AE; TSS: alternative 5' first exon; TTS: alternative 3' last exon.

doi:10.1371/journal.pone.0147950.g002

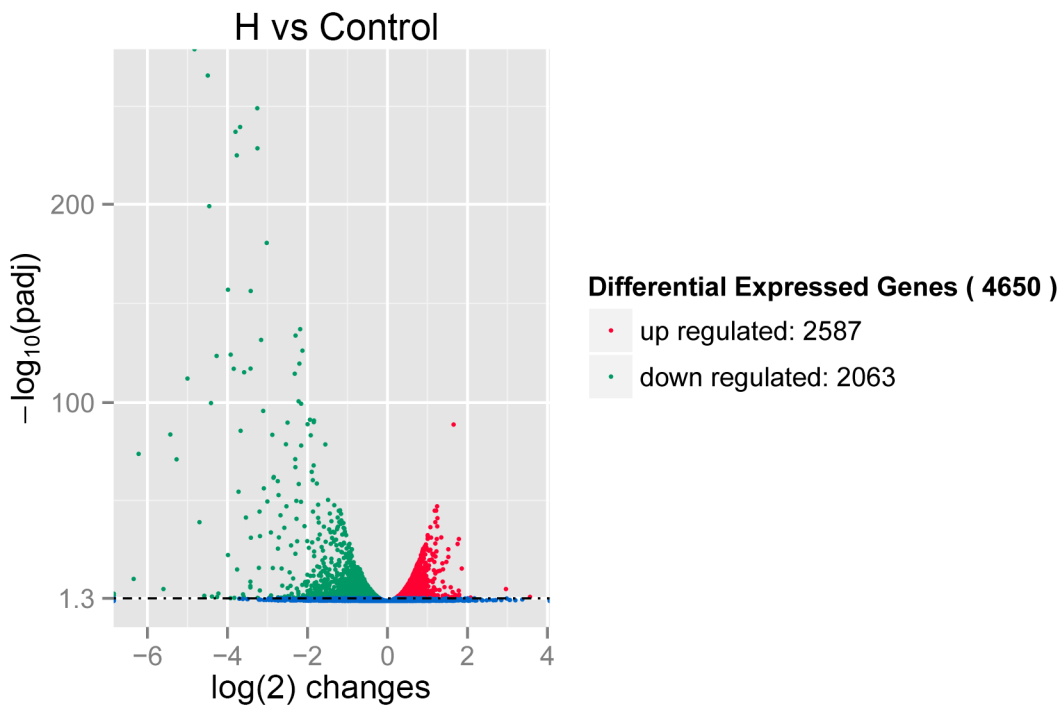


**Fig 3. Volcano plot of differentially expressed genes.** Each point represents one gene; red color indicates upregulation and green indicates downregulation.

doi:10.1371/journal.pone.0147950.g003

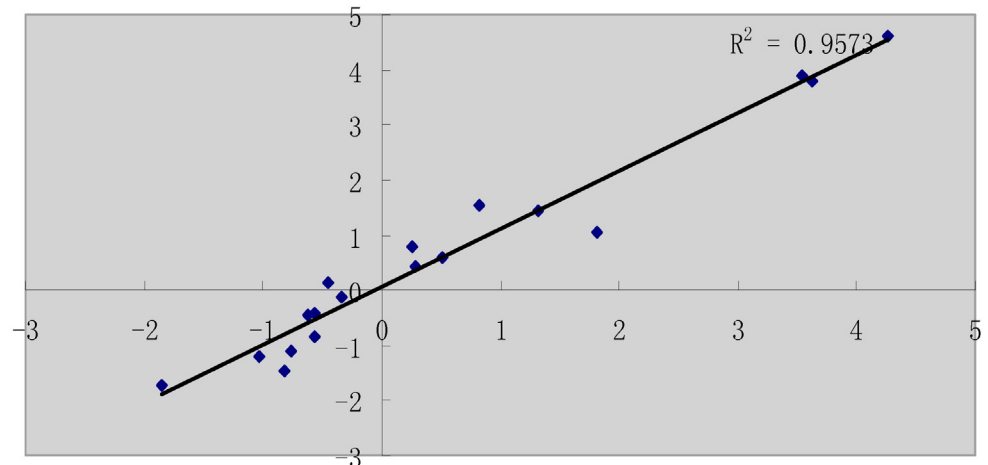


**Fig 4. Validation of the RNA-Seq approach using qPCR.** Eighteen genes that were differentially expressed between the H and control groups (10 upregulated and 8 downregulated) were selected. Their levels of expression were quantified by qRT-PCR analysis. The log<sub>2</sub> changes in expression for the qRT-PCR and RNA-Seq data were closely correlated ( $r^2 = 0.9573$ ;  $p < 0.01$ ), confirming the accuracy of the RNA-Seq approach for quantification.

doi:10.1371/journal.pone.0147950.g004

## GO and KEGG enrichment analyses of differentially expressed genes

GO enrichment analysis of differentially expressed genes was performed using the GOrse R package. GO terms with corrected  $P < 0.05$  were considered significantly enriched in differentially expressed genes. Genes were categorized into 10,563 GO terms within three domains: 'biological process', 'cellular component', and 'molecular function' (Fig 5). In the 'biological process' domain, the GO terms with highest enrichment of differentially expressed genes were 'regulation of response to stimulus', 'response to stress', and 'macromolecule localization'. In the cell 'component domain', terms with highest enrichment were 'intracellular', 'cell', and 'cell part'. We also observed a high percentage of differentially expressed genes assigned to 'intracellular signal transduction', 'regulation of signal transduction', and 'regulation of cell communication'. Alternatively, few genes were assigned to terms such as 'establishment of nucleus localization' and 'fibronectin binding'.

We analyzed the biological pathways that were active in our samples. Genes were mapped to the reference pathways in the KEGG and assigned to 152 KEGG pathways (S1 File). A few pathways, including the cytokine-cytokine receptor interaction pathway, MAPK signaling pathway, metabolic pathways, and regulation of the actin cytoskeleton pathway, contained large numbers of differentially expressed genes, while others, such as sulfur metabolism, contained only a few (Fig 6).

## Discussion

A previous gene expression profiling study of infarcted myocardial tissue with signs of oxidative stress reported over a thousand differentially expressed genes, of which hundreds were sensitive to administration of antioxidants [20]. Furthermore, gene chip studies have shown that direct application of cytotoxic concentrations of H<sub>2</sub>O<sub>2</sub> or other oxidants results in the up- or downregulation of hundreds to thousands of known protein-encoding genes [21, 22]. In present study, the first using RNA-Seq to examine gene expression changes during H<sub>2</sub>O<sub>2</sub>-induced oxidative stress and apoptosis in chicken myocardial cells, we identified over 6000 differentially expressed genes. This vast number reflects not only proteins directly related to apoptosis, but

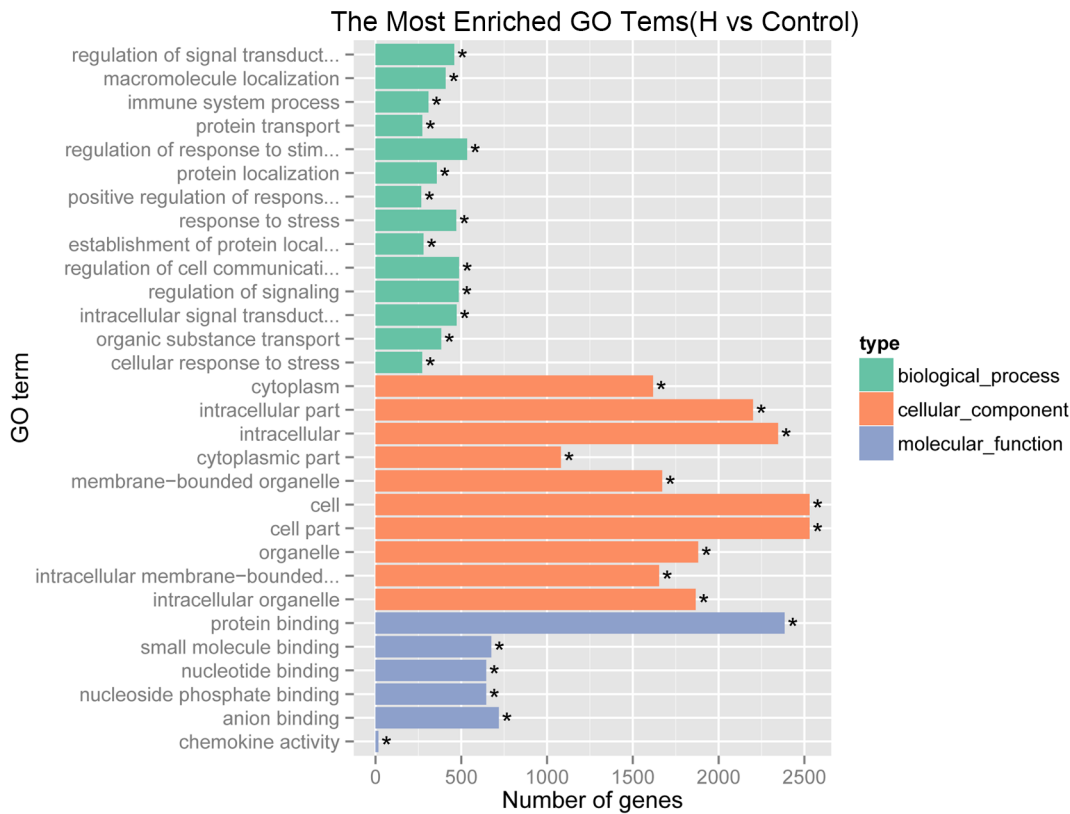


**Fig 5. Results of GO enrichment analyses, including biological process, cellular component, and molecular function.**

doi:10.1371/journal.pone.0147950.g005

also myriad protein expression cascades involved in mitochondrial function, cell cycle regulation, DNA repair, protein translation and turnover, and antioxidant responses [23–26]. Genes transiently induced in the early phase of oxidative stress include a variety of redox-sensitive transcription factors that in turn activate multiple downstream targets [21, 27]. Thus, these numbers may be underestimates as expression levels of many genes likely return to baseline before profiling [22]. Transient early expression also explains the variation in expression profiles among cell types and oxidative stress induction paradigms. Despite this variation, the assembled annotated transcriptomes reported in these studies provide a valuable resource for understanding myocardial cell apoptosis and other cellular changes induced by oxidative stress. In contrast to many previous studies, however, the RNA-seq profiling presented here revealed over 2000 novel genes, underscoring the utility of this expression profiling method for identifying genes not previously implicated in cytotoxic responses by other profiling techniques.

### The classification of novel genes

After sequencing, a total of 2,160 novel genes were found. We blasted these genes and investigated open reading frames (ORFs) using ORF Finder [http://www.ncbi.nlm.nih.gov/projects/gorf/]. Most novel genes were noncoding RNAs, including many long noncoding RNAs (LncRNAs), suggesting that LncRNAs are involved in the regulation of apoptosis and other signaling processes evoked by H<sub>2</sub>O<sub>2</sub>. Indeed, multiple LncRNAs have been implicated in chronic cardiovascular diseases, myocardial cell proliferation, and cell death [28, 29].



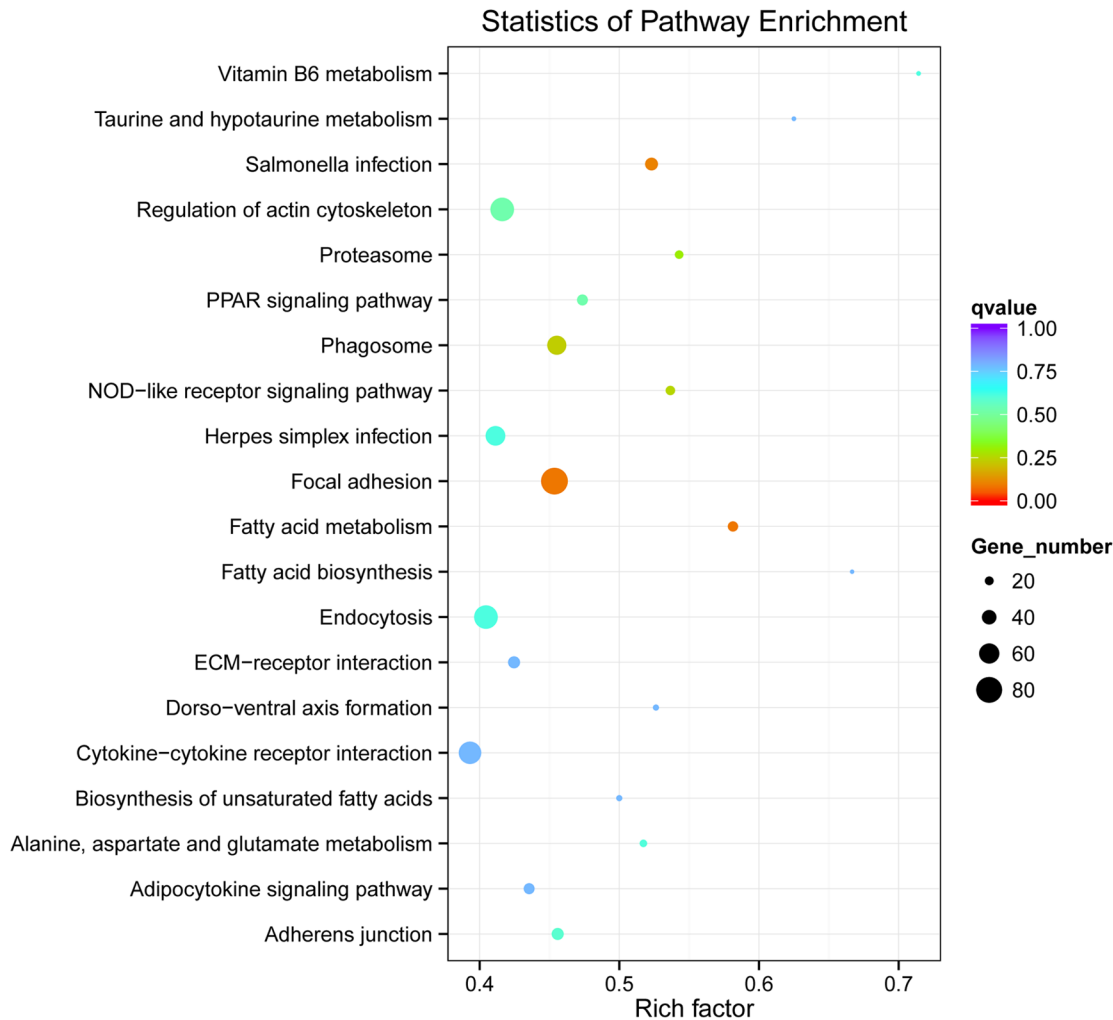


**Fig 6. Statistics of KEGG enrichment.** The size of each point indicates the number of differentially expressed genes in that pathway, and the color of each point indicates the q-value (adjusted p value). A higher enrichment factor indicates a greater degree of enrichment.

doi:10.1371/journal.pone.0147950.g006

### Screening pathways related to hydrogen peroxide toxicity

The differentially expressed genes were mapped to reference pathways in the KEGG and assigned to 152 KEGG pathways, including many metabolic and signaling pathways not directly related to apoptosis. For instance, within the metabolism domain, H<sub>2</sub>O<sub>2</sub> altered expression of genes involved in 'Fatty acid metabolism', 'Alanine, aspartate and glutamate metabolism', 'Biosynthesis of unsaturated fatty acids', 'Protein processing in endoplasmic reticulum', 'Vitamin B6 metabolism', 'Pyruvate metabolism', and 'Pantothenate and CoA biosynthesis'. We conclude that H<sub>2</sub>O<sub>2</sub> has broad effects on cell metabolism, mainly on fatty acid, alanine, aspartate, and glutamate metabolism. It also affects 'cell biosynthesis', particularly protein processing and fatty acid synthesis, possibly as part of the repair response for mitigating H<sub>2</sub>O<sub>2</sub>-induced oxidative damage to proteins and lipid membranes.

Exposure to H<sub>2</sub>O<sub>2</sub> also activated the 'PPAR signaling pathway', 'Adipocytokine signaling pathway', 'TGF-beta signaling pathway', 'Toll-like receptor signaling pathway', 'MAPK signaling pathway', 'p53 signaling pathway', and 'Wnt signaling pathway'. Most of these pathways

are known regulators of apoptosis, such as 'MAPK signaling pathway' and 'p53 signaling pathway'. The *Wnt* signaling isoform *WNT5A* enhanced H<sub>2</sub>O<sub>2</sub>-resistance in fibroblasts [25], so *Wnt* pathway activation may represent a cytoprotective response. In contrast, *NF-κB* is a well known stress response gene linked to cell death, at least when stress is severe. Glucocorticoid inhibition of *NF-κB* in macrophages blocked H<sub>2</sub>O<sub>2</sub>-induced apoptosis [30]. Alternatively, *MAPKs* are broadly cytoprotective. The balance between *NF-κB* and *MAPK* signaling may determine cell fate (apoptosis vs. survival) under oxidative stress [31].

In addition, H<sub>2</sub>O<sub>2</sub> altered the expression of genes associated with 'Regulation of actin cytoskeleton' and 'cell cycle', possible reflecting the changes in morphology and proliferation rate in response to H<sub>2</sub>O<sub>2</sub> exposure. Several previous studies have reported modulation of cell cycle regulators and reduced proliferation concomitant with the antioxidant response [24, 25].

GO enrichment analysis indicated that many differentially expressed genes are associated with 'cellular response to chemical stimulus', 'response to stress', 'regulation of signal transduction', 'cell migration', 'response to oxygen levels', and 'protein metabolic process', in line with the KEGG analysis.

### Differential expression of apoptosis regulators

We examined the expression levels of *caspase-2*, *caspase-8*, *caspase-9*, and *caspase-10* [32–34] and of the effector caspases *caspase-3*, *caspase-6*, and *caspase-7* [35, 36]. Our results showed that apoptosis initiation predominantly relies on *caspase-8* and *caspase-9* upregulation, leading to *caspase-3* activation, so H<sub>2</sub>O<sub>2</sub>-induced apoptosis in chicken cardiomyocytes depends on the canonical apoptosis pathway. We also examined the expression of several apoptosis repressors, including *bcl-2*, *CFLAR*, *CAAP1*, *IAP*, *BFAR*, *TRIA1*, *API5*, and *CAPP1* [37–41]. By comparing expression levels in the apoptosis group with those in the control group, we found that the repression of apoptosis may rely on *API5* and *TRIA1*. In addition, GO enrichment analysis identified two novel genes that may be involved in apoptosis repression. However, we also found that other anti-apoptosis genes, such as *IAP* and *BFAR*, were significantly downregulated following H<sub>2</sub>O<sub>2</sub> treatment. Other differentially expressed genes are less direct regulators of apoptosis. Products of the downregulated *EGLN* gene family, hypoxia-inducible factor prolyl hydrolases, are ubiquitination-dependent suppressors of hypoxia-inducible factors (*HIFs*), transcription factors that induce a variety of cytoprotective responses during oxidative stress [42]. Downregulation of *EGLN* genes and concomitant enhancement of *HIF* activity could serve to protect against H<sub>2</sub>O<sub>2</sub>-induced oxidative stress. However, H<sub>2</sub>O<sub>2</sub> also downregulated the forkhead family transcription factor *FOXO3*, which is known to upregulate antioxidant enzymes, including catalase [43]. Thus, H<sub>2</sub>O<sub>2</sub> activated both cell death and cytoprotective pathways (also including the X-linked inhibitor of apoptosis protein (*XIAP*)).

### Differential expression of cell cycle regulators

In addition to apoptosis-associated genes, H<sub>2</sub>O<sub>2</sub> altered expression of genes associated with cell cycle regulation and DNA damage. Genes regulating the cell cycle, such as *CDK4-6*, *Bax*, *TP53*, *CDC2*, and *DK1* [44–46] were all significantly differentially expressed, suggesting that H<sub>2</sub>O<sub>2</sub> may reduce the cardiomyocyte population in the embryo by suppressing proliferation.

### RNA-seq is suitable for using in toxicology research

While RNA-seq is frequently used to screen differentially expressed genes and novel genes, it has rarely been employed in toxicology research. Our work demonstrates the utility of RNA-Seq for screening of toxicological responses in cells and tissues. Further studies to assess the applicability of RNA-seq to in vivo toxicology are warranted.

## Conclusion

Cytotoxic effects of hydrogen peroxide have been reported in many studies, but the full panoply of differentially expressed genes had not been examined by RNA-seq. We used RNA-Seq to identify genes differentially expressed in cardiomyocytes undergoing H<sub>2</sub>O<sub>2</sub>-induced apoptosis. Sequencing identified 19,268 known genes and 2,160 novel genes, of which 4,650 were significantly differentially expressed between control and H<sub>2</sub>O<sub>2</sub>-treated cells. Apoptosis was associated with upregulation of *caspase-8*, *caspase-9*, and *caspase-3*, and downregulation of anti-apoptotic genes *API5* and *TRIA1*. However, H<sub>2</sub>O<sub>2</sub> exposure was also associated with changes in many genes associated with metabolic and signaling pathways. Hydrogen peroxide appears to have myriad effects on cell biosynthesis (protein processing, fatty acid synthesis), morphology, and the cell cycle. Furthermore, this study demonstrates the potential of RNA-seq for molecular toxicology research.

## Supporting Information

**S1 Fig. Culture and identification of primary cardiomyocyte.** (A) Untreated primary cardiomyocytes (100×). (B) Primary cardiomyocytes stained by DAPI after H<sub>2</sub>O<sub>2</sub>-induced apoptosis (100×), (C) Immunocytochemical staining showing abundant  $\alpha$ -actin (400×) in chicken cardiomyocytes. (D) Control fibroblasts showing no  $\alpha$ -actin immunoreactivity (400×). (TIF)

**S1 File. KEGG enrichment of differential expressed genes.** (XLS)

**S1 Table. Alignment between reads and reference genome.** (DOC)

**S2 Table. Primers used for qRT-PCR analysis.** (DOC)

## Acknowledgments

Our work was supported by preliminary research project of Huazhong agricultural university [52209–814112]. The funders had no role in study design, data collection and analysis, decision to publish, or preparation of the manuscript. The authors thank Xiaona Zhang and Xiang Cui at NOVogene (Beijing, China) for assistance with the Illumina sequencing. Dr. Jianfeng Gao is thanked for assistance with the cell treatments.

## Author Contributions

Conceived and designed the experiments: CW DG. Performed the experiments: CW JX. Analyzed the data: JX YL. Contributed reagents/materials/analysis tools: YL. Wrote the paper: CW JX.

## References

1. Kerr JF, Wyllie AH, Currie AR. Apoptosis: a basic biological phenomenon with wide-ranging implications in tissue kinetics. *Br J Cancer* 1972; 26: 239–257. PMID: [4561027](#)
2. Gaballa M A, Goldman S. Ventricular remodeling in heart failure. *J Card Fail.* 2002; 8: 476–485.
3. Park K-J, Kim Y-J, Kim J, Kim SM, Lee SY, Bae J-W, et al. Protective effects of peroxiredoxin on hydrogen peroxide induced oxidative stress and apoptosis in cardiomyocytes. *Korean Circ J.* 2012; 42: 23–32. doi: [10.4070/kcj.2012.42.1.23](#) PMID: [22363380](#)

4. Li R, Yan G, Li Q, Sun H, Hu Y, Sun J, Xu B. MicroRNA-145 protects cardiomyocytes against hydrogen peroxide (H<sub>2</sub>O<sub>2</sub>)-induced apoptosis through targeting the mitochondria apoptotic pathway. *PLoS One* 2012; 7: e44907. doi: [10.1371/journal.pone.0044907](https://doi.org/10.1371/journal.pone.0044907) PMID: [23028672](https://pubmed.ncbi.nlm.nih.gov/23028672/)
5. Suzuki T, Yang J. Hydrogen peroxide activation of ERK5 confers resistance to Jurkat cells against apoptosis induced by the extrinsic pathway. *Biochem Biophys Res Commun.* 2014; 444: 248–253. doi: [10.1016/j.bbrc.2014.01.058](https://doi.org/10.1016/j.bbrc.2014.01.058) PMID: [24462874](https://pubmed.ncbi.nlm.nih.gov/24462874/)
6. Tamim S, Vo DT, Uren PJ, Qiao M, Bindewald E, Kasprzak WK, et al. Genomic analyses reveal broad impact of miR-137 on genes associated with malignant transformation and neuronal differentiation in glioblastoma cells. *PLoS One* 2014; 9: e85591. doi: [10.1371/journal.pone.0085591](https://doi.org/10.1371/journal.pone.0085591) PMID: [24465609](https://pubmed.ncbi.nlm.nih.gov/24465609/)
7. Olkowski AA Pathophysiology of heart failure in broiler chickens: structural, biochemical, and molecular characteristics. *Poult Sci.* 2007; 86: 999–1005. PMID: [17435038](https://pubmed.ncbi.nlm.nih.gov/17435038/)
8. Connell S, Meade KG, Allan B, Lloyd AT, Kenny E, Cormican P, et al. Avian resistance to *Campylobacter jejuni* colonization is associated with an intestinal immunogene expression signature identified by mRNA sequencing. *PLoS One* 2012; 7: e40409. doi: [10.1371/journal.pone.0040409](https://doi.org/10.1371/journal.pone.0040409) PMID: [22870198](https://pubmed.ncbi.nlm.nih.gov/22870198/)
9. Gruss-Fischer T, Fabian I Protection by ascorbic acid from denaturation and release of cytochrome c, alteration of mitochondrial membrane potential and activation of multiple caspases induced by H<sub>2</sub>O<sub>2</sub> in human leukemia cells. *Biochem Pharmacol.* 2002; 63: 1325–1335. PMID: [11960609](https://pubmed.ncbi.nlm.nih.gov/11960609/)
10. Fukuda K. Current status of myocardial regeneration and cell transplantation. *Future Cardiol.* 2005; 1: 167–175. doi: [10.1517/14796678.1.2.167](https://doi.org/10.1517/14796678.1.2.167) PMID: [19804162](https://pubmed.ncbi.nlm.nih.gov/19804162/)
11. Takeuchi T. Regulation of cardiomyocyte proliferation during development and regeneration. *Dev Growth Differ.* 2014; 56: 402–409. doi: [10.1111/dgd.12134](https://doi.org/10.1111/dgd.12134) PMID: [24738847](https://pubmed.ncbi.nlm.nih.gov/24738847/)
12. Solaini G, Harris DA. Biochemical dysfunction in heart mitochondria exposed to ischaemia and reperfusion. *Biochem J.* 2005; 390: 377–394. PMID: [16108756](https://pubmed.ncbi.nlm.nih.gov/16108756/)
13. DeHaan RL. Development of form in the embryonic heart, An experimental approach. *Circulation* 1967; 35: 821–833. PMID: [6021773](https://pubmed.ncbi.nlm.nih.gov/6021773/)
14. Mortazavi A, Williams BA, McCue K, Schaeffer L, Wold B. Mapping and quantifying mammalian transcriptomes by RNA-Seq. *Nat Methods* 2008; 5: 621–628. doi: [10.1038/nmeth.1226](https://doi.org/10.1038/nmeth.1226) PMID: [18516045](https://pubmed.ncbi.nlm.nih.gov/18516045/)
15. Jiang B, Xiao W, Shi Y, Liu M, Xiao X. Heat shock pretreatment inhibited the release of Smac/DIABLO from mitochondria and apoptosis induced by hydrogen peroxide in cardiomyocytes and C2C12 myogenic cells. *Cell Stress Chaperones* 2005; 10: 252–262. PMID: [16184770](https://pubmed.ncbi.nlm.nih.gov/16184770/)
16. Akazawa Y, Isomoto H, Matsushima K, Kanda T, Minami H, Yamaguchi N, et al. Endoplasmic reticulum stress contributes to *Helicobacter pylori* VacA-induced apoptosis. *PLoS One* 2012; 8: e82322.
17. Renfro DP, McIntosh BK, Venkatraman A, Siegele DA, Hu JC. GONUTS: the Gene Ontology Normal Usage Tracking System. *Nucleic Acids Res.* 2012; 40: D1262–D1269. doi: [10.1093/nar/gkr907](https://doi.org/10.1093/nar/gkr907) PMID: [22110029](https://pubmed.ncbi.nlm.nih.gov/22110029/)
18. Mao X, Cai T, Olyarchuk JG, Wei L. Automated genome annotation and pathway identification using the KEGG Orthology (KO) as a controlled vocabulary. *Bioinformatics* 2005; 21: 3787–3793. PMID: [15817693](https://pubmed.ncbi.nlm.nih.gov/15817693/)
19. Kanehisa M, Araki M, Goto S, Hattori M, Hirakawa M, Itoh M, et al. KEGG for linking genomes to life and the environment. *Nucleic Acids Res.* 2008; 36: D480–D484. PMID: [18077471](https://pubmed.ncbi.nlm.nih.gov/18077471/)
20. Zhao W, Zhao T, Chen Y, Qu Y, Gerling IC, Sun Y. Modification of oxidative stress on gene expression profiling in the rat infarcted heart. *Mol Cell Biochem.* 2013; 379: 243–253. doi: [10.1007/s11010-013-1646-2](https://doi.org/10.1007/s11010-013-1646-2) PMID: [23716180](https://pubmed.ncbi.nlm.nih.gov/23716180/)
21. Clerk A, Kemp TJ, Zoumpoulidou G, Sugden PH. Cardiac myocyte gene expression profiling during H<sub>2</sub>O<sub>2</sub>-induced apoptosis. *Physiol Genomics.* 2007; 29: 118–127. PMID: [17148688](https://pubmed.ncbi.nlm.nih.gov/17148688/)
22. Briedé JJ, van Delft JM, de Kok TM, van Herwijnen MH, Maas LM, Gottschalk RW, Kleinjans JC. Global gene expression analysis reveals differences in cellular responses to hydroxyl- and superoxide anion radical-induced oxidative stress in caco-2 cells. *Toxicol Sci.* 2010; 114: 193–203. doi: [10.1093/toxsci/kfp309](https://doi.org/10.1093/toxsci/kfp309) PMID: [20044591](https://pubmed.ncbi.nlm.nih.gov/20044591/)
23. Shibamura M, Inoue A, Ushida K, Uchida T, Ishikawa F, Mori K, Nose K. Importance of mitochondrial dysfunction in oxidative stress response: A comparative study of gene expression profiles. *Free Radic Res.* 2011; 45: 672–680. doi: [10.3109/10715762.2011.564169](https://doi.org/10.3109/10715762.2011.564169) PMID: [21391894](https://pubmed.ncbi.nlm.nih.gov/21391894/)
24. Chua PJ, Yip GW, Bay BH. Cell cycle arrest induced by hydrogen peroxide is associated with modulation of oxidative stress related genes in breast cancer cells. 2009; 234: 1086–1094.
25. Vuga LJ, Ben-Yehudah A, Kovkarova-Naumovski E, Oriss T, Gibson KF, Feghali-Bostwick C, Kaminski N. WNT5A is a regulator of fibroblast proliferation and resistance to apoptosis. *Am J Respir Cell Mol Biol.* 2009; 41: 583–589. doi: [10.1165/rcmb.2008-0201OC](https://doi.org/10.1165/rcmb.2008-0201OC) PMID: [19251946](https://pubmed.ncbi.nlm.nih.gov/19251946/)

26. Zhang J, Song R, Li Y, Feng J, Peng L, Li J. Integration of microarray profiles associated with cardiomyopathy and the potential role of Ube3a in apoptosis. *Mol Med Rep.* 2014; 9: 621–625. doi: [10.3892/mmr.2013.1848](https://doi.org/10.3892/mmr.2013.1848) PMID: [24337433](https://pubmed.ncbi.nlm.nih.gov/24337433/)
27. Platel A, Gervais V, Sajot N, Nessler F, Marzin D, Claude N. Study of gene expression profiles in TK6 human cells exposed to DNA-oxidizing agents. *Mutat Res.* 2010; 689: 21–49. doi: [10.1016/j.mrfmmm.2010.04.004](https://doi.org/10.1016/j.mrfmmm.2010.04.004) PMID: [20466008](https://pubmed.ncbi.nlm.nih.gov/20466008/)
28. Uchida S, Dimmeler S. Long noncoding RNAs in cardiovascular diseases. *Circ Res.* 2015; 116: 737–750. doi: [10.1161/CIRCRESAHA.116.302521](https://doi.org/10.1161/CIRCRESAHA.116.302521) PMID: [25677520](https://pubmed.ncbi.nlm.nih.gov/25677520/)
29. Piccoli MT, Gupta SK, Thum T. Noncoding RNAs as regulators of cardiomyocyte proliferation and death. *J Mol Cell Cardiol.* 2015 pii: S0022-2828(15)00039-5.
30. Fong CC, Zhang Y, Zhang Q, Tzang CH, Fong WF, Wu RS, Yang M. Dexamethasone protects RAW264.7 macrophages from growth arrest and apoptosis induced by H<sub>2</sub>O<sub>2</sub> through alteration of gene expression patterns and inhibition of nuclear factor-kappa B (NF-kappaB) activity. *Toxicology* 2007; 236: 16–28. PMID: [17499901](https://pubmed.ncbi.nlm.nih.gov/17499901/)
31. Choi CH, Xu H, Bark H, Lee TB, Yun J, Kang SI, Oh YK. Balance of NF-kappaB and p38 MAPK is a determinant of radiosensitivity of the AML-2 and its doxorubicin-resistant cell lines. *Leuk Res.* 2007; 31: 1267–1276. PMID: [17218010](https://pubmed.ncbi.nlm.nih.gov/17218010/)
32. Grossmann J, Walther K, Artinger M, Kiessling S, Schölmerich J. Apoptotic signaling during initiation of detachment-induced apoptosis ("anoikis") of primary human intestinal epithelial cells. *Cell Growth Differ.* 2001; 12: 147–155. PMID: [11306515](https://pubmed.ncbi.nlm.nih.gov/11306515/)
33. Mueller T, Voigt W, Simon H, Fruehauf A, Bulankin A, Grothey A, Schmoll HJ. Failure of activation of caspase-9 induces a higher threshold for apoptosis and cisplatin resistance in testicular cancer. *Cancer Res.* 2003; 63: 513–521. PMID: [12543810](https://pubmed.ncbi.nlm.nih.gov/12543810/)
34. Chang GC, Hsu SL, Tsai JR, Liang FP, Lin SY, Sheu GT, Chen CY. Molecular mechanisms of ZD1839-induced G1-cell cycle arrest and apoptosis in human lung adenocarcinoma A549 cells. *Biochem Pharmacol.* 2004; 68: 1453–1464. PMID: [15345335](https://pubmed.ncbi.nlm.nih.gov/15345335/)
35. Gregoli PA, Bondurant MC. Function of caspases in regulating apoptosis caused by erythropoietin deprivation in erythroid progenitors. *J Cell Physiol.* 1999; 178: 133–143. PMID: [10048577](https://pubmed.ncbi.nlm.nih.gov/10048577/)
36. Lee CJ, Liao CL, Lin YL. Flavivirus activates phosphatidylinositol 3-kinase signaling to block caspase-dependent apoptotic cell death at the early stage of virus infection. *J Virol.* 2005; 79: 8388–8399. PMID: [15956583](https://pubmed.ncbi.nlm.nih.gov/15956583/)
37. Chao DT, Linette GP, Boise LH, White LS, Thompson CB, Korsmeyer SJ. Bcl-XL and Bcl-2 repress a common pathway of cell death. *J Exp Med.* 1995; 182: 821–828. PMID: [7650488](https://pubmed.ncbi.nlm.nih.gov/7650488/)
38. Zhang Y, Johansson E, Miller ML, Jänicke RU, Ferguson DJ, Plas D, et al. Identification of a conserved anti-apoptotic protein that modulates the mitochondrial apoptosis pathway. *PLoS One* 2011; 6: e25284. doi: [10.1371/journal.pone.0025284](https://doi.org/10.1371/journal.pone.0025284) PMID: [21980415](https://pubmed.ncbi.nlm.nih.gov/21980415/)
39. Furukawa J, Miyake H, Fujisawa M. Upregulation of anti-apoptotic gene. *Nihon Rinsho* 2011; 69 Suppl 5:117–120. PMID: [22207954](https://pubmed.ncbi.nlm.nih.gov/22207954/)
40. Fortin A, MacLaurin JG, Arbour N, Cregan SP, Kushwaha N, Callaghan SM, et al. The proapoptotic gene SIVA is a direct transcriptional target for the tumor suppressors p53 and E2F1. *J Biol Chem.* 2004; 279: 28706–28714. PMID: [15105421](https://pubmed.ncbi.nlm.nih.gov/15105421/)
41. Ewen ME, Oliver CJ, Sluss HK, Miller SJ, Peeper DS. p53-dependent repression of CDK4 translation in TGF-beta-induced G1 cell-cycle arrest. *Genes Dev.* 1995; 9: 204–217. PMID: [7851794](https://pubmed.ncbi.nlm.nih.gov/7851794/)
42. Karuppagounder SS, Ratan RR. Hypoxia-inducible factor prolyl hydroxylase inhibition: robust new target or another big bust for stroke therapeutics? *J Cereb Blood Flow Met.* 2012; 32:1347–1361.
43. Tan W-Q, Wang K, Lv D-Y, Li P-F. Foxo3a inhibits cardiomyocyte hypertrophy through transactivating catalase. *J Biol Chem.* 2008; 283: 29730–29739. doi: [10.1074/jbc.M805514200](https://doi.org/10.1074/jbc.M805514200) PMID: [18772130](https://pubmed.ncbi.nlm.nih.gov/18772130/)
44. Fry DW, Bedford DC, Harvey PH. Cell cycle and biochemical effects of PD 0183812. A potent inhibitor of the cyclin D-dependent kinases CDK4 and CDK6. *J Biol Chem.* 2001; 276: 16617–16623. PMID: [11278443](https://pubmed.ncbi.nlm.nih.gov/11278443/)
45. Wu J, Feng Y, Xie D, Li X, Xiao W, Tao D, et al. Unscheduled CDK1 activity in G1 phase of the cell cycle triggers apoptosis in X-irradiated lymphocytic leukemia cells. *Cell Mol Life Sci.* 2006; 63: 2538–2545. PMID: [17013563](https://pubmed.ncbi.nlm.nih.gov/17013563/)
46. Skomedal H, Kristensen GB, Nesland JM, Borresen-Dale AL, Trope C, Holm R. TP53 alterations in relation to the cell cycle-associated proteins p21, cyclin D1, CDK4, RB, MDM2, and EGFR in cancers of the uterine corpus. *J Pathol.* 1999; 187: 556–562. PMID: [10398121](https://pubmed.ncbi.nlm.nih.gov/10398121/)